DUNLAP INSTITUTE
for ASTRONOMY & ASTROPHYSICS

Pon et al. (2014)

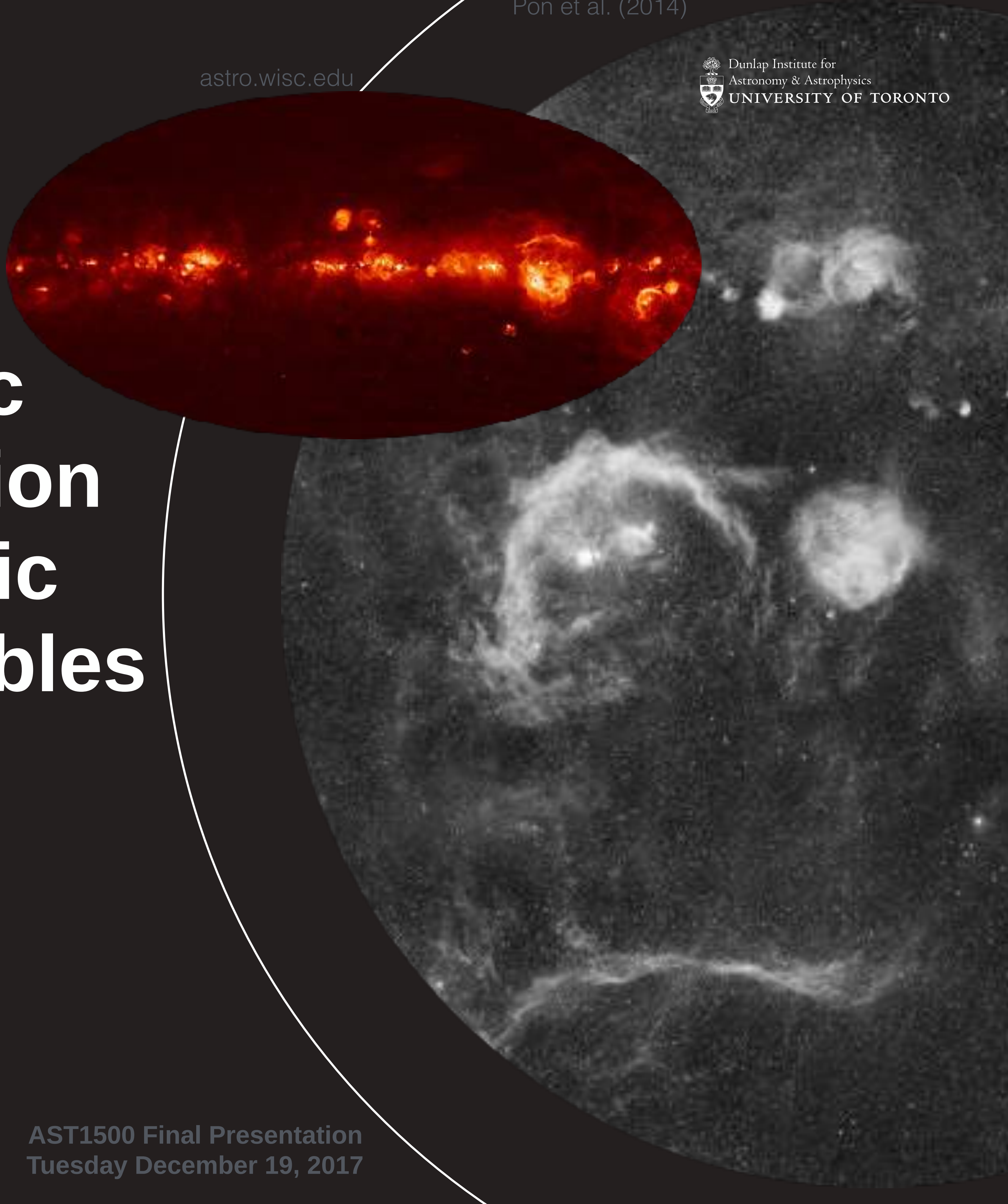

astro.wisc.edu

Dunlap Institute for Astronomy & Astrophysics
UNIVERSITY OF TORONTO

A Magneto-ionic Radio Polarization Study of Galactic Loops and Bubbles

Jessica Campbell
Supervised by Bryan Gaensler

AST1500 Final Presentation
Tuesday December 19, 2017

Radio Loops in the Milky Way Galaxy

- Some of the largest features in the sky
- Studied for >50 years; origin still unclear
- Spectral index suggests non-thermal emission mechanism
- Seen in polarization (starlight, radio)

408 MHz synchrotron emission (Haslam)

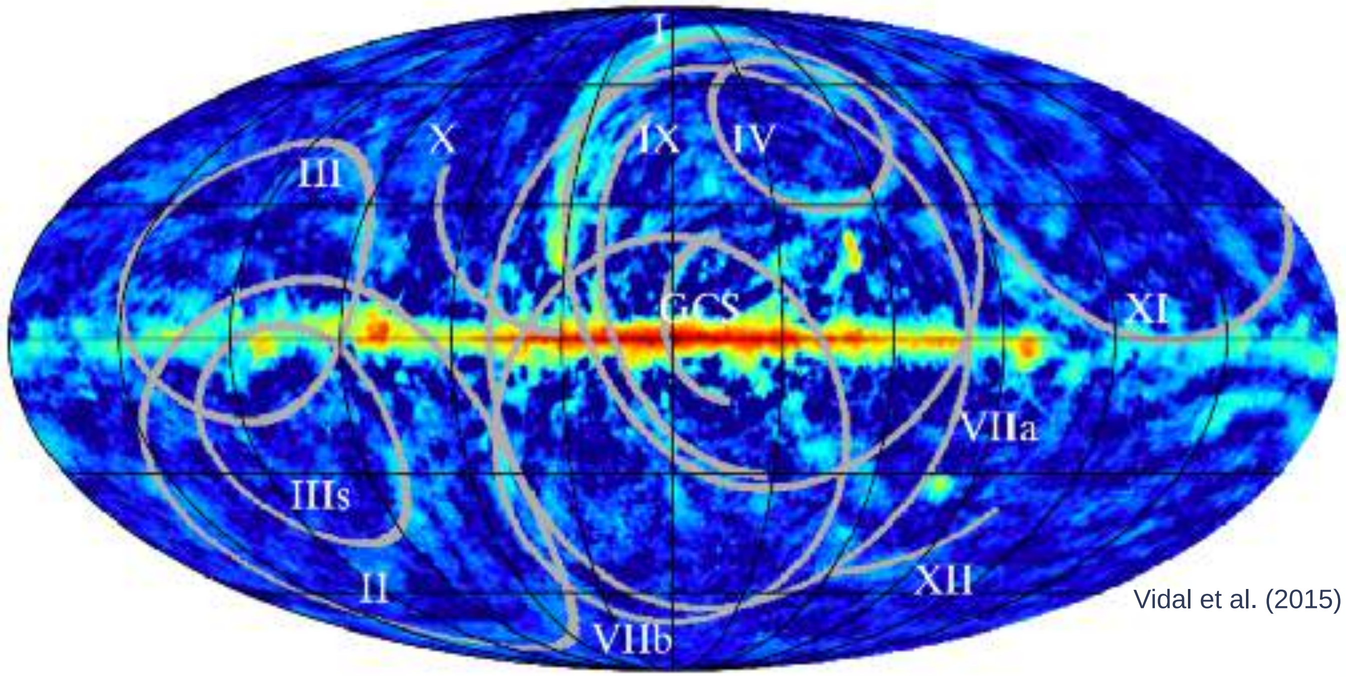

Vidal et al. (2015)

22.7 GHz polarization intensity (WMAP)

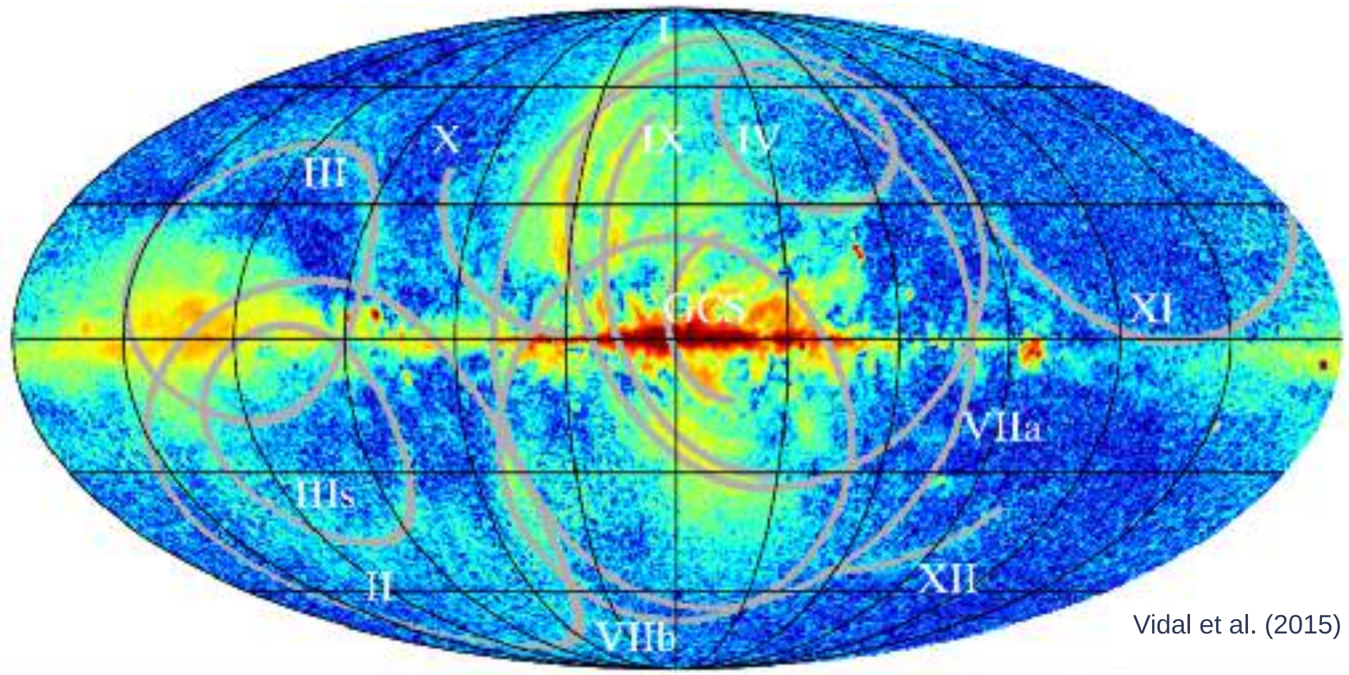

Vidal et al. (2015)

Synchrotron emission mechanism

- Relativistic electrons spiral along local magnetic fields
- Generates highly collimated linearly polarized radiation

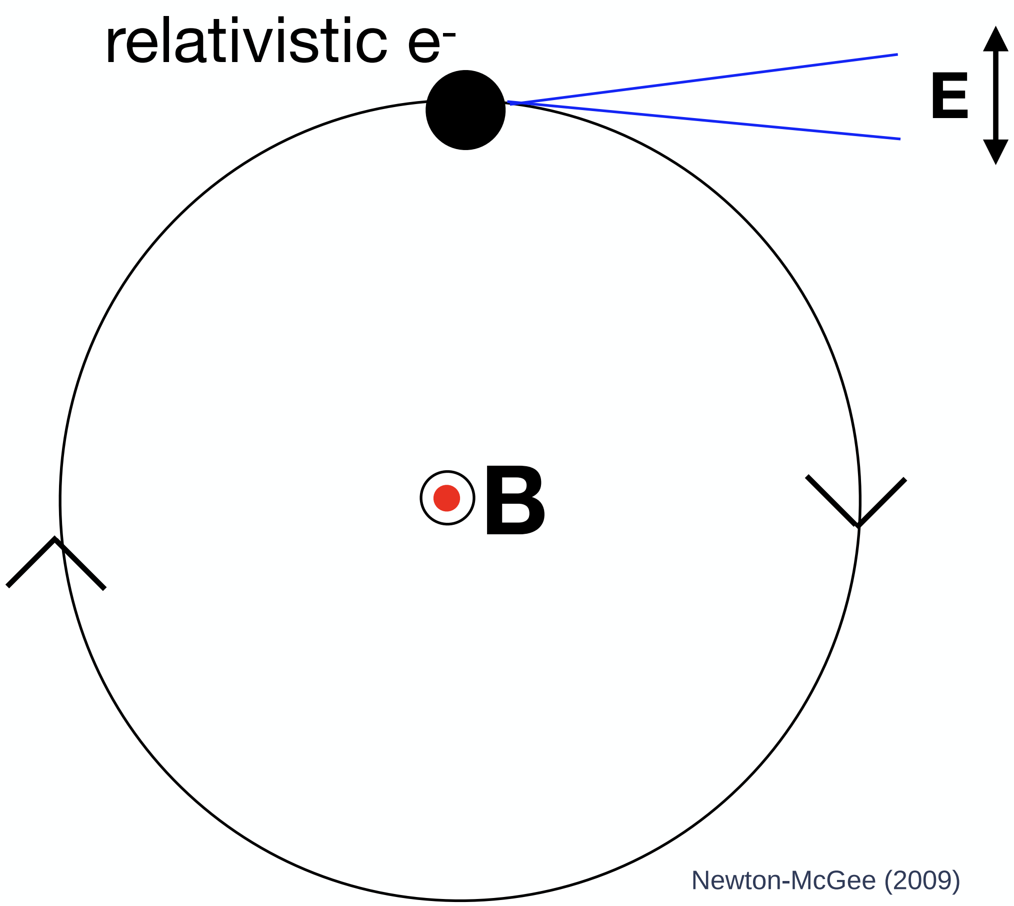

Newton-McGee (2009)

Synchrotron emission mechanism

- Relativistic electrons spiral along local magnetic fields
- Generates highly collimated linearly polarized radiation
- Degree of polarization depends on spectral index:

$$p(\alpha) = \frac{3\alpha + 3}{3\alpha + 7}$$

Le Roux (1961)

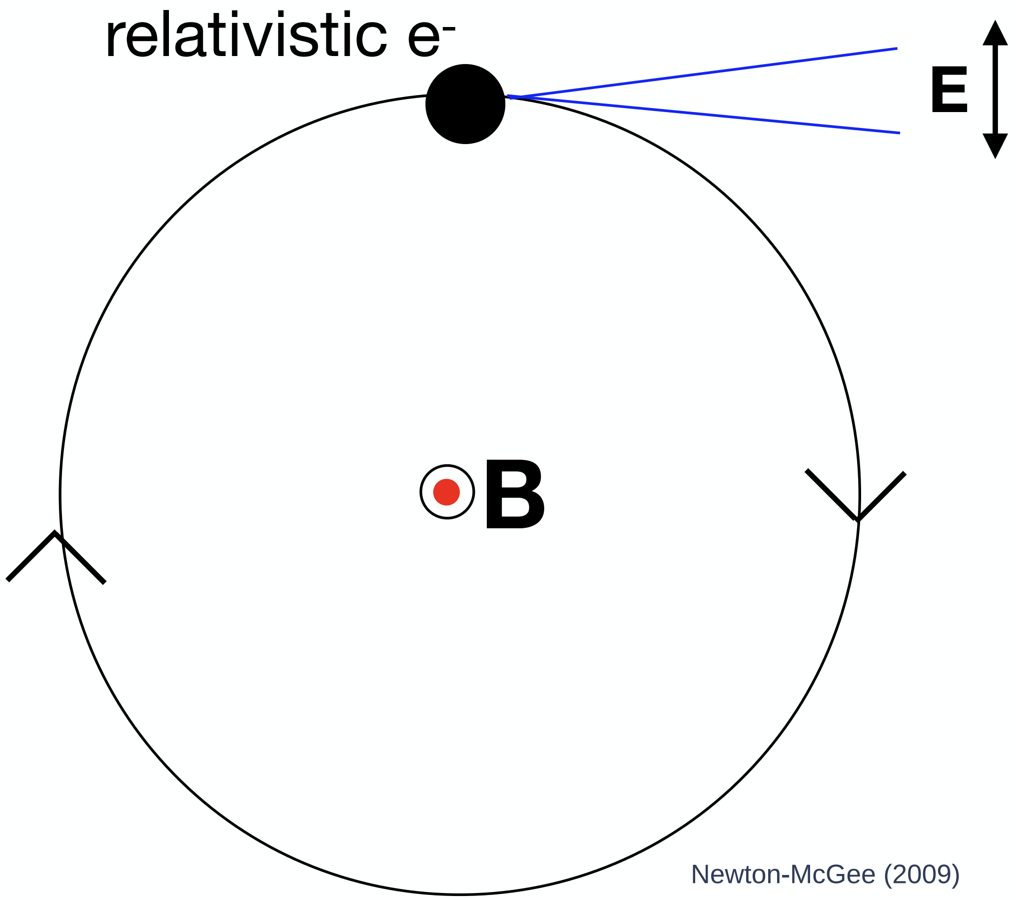

Newton-McGee (2009)

- For typical spectral index of cosmic ray electrons,

$$p(5/3) \approx 67\%$$

Westfold (1959)

- Depolarization effects prevents such high degrees of polarization

Superbubbles in the Milky Way Galaxy

- Have also been studied for ~50 years with
- Individual bubbles OB-driven stellar winds, radiation fields and SNe
- Overlapping effects from OB associations results in “superbubbles”

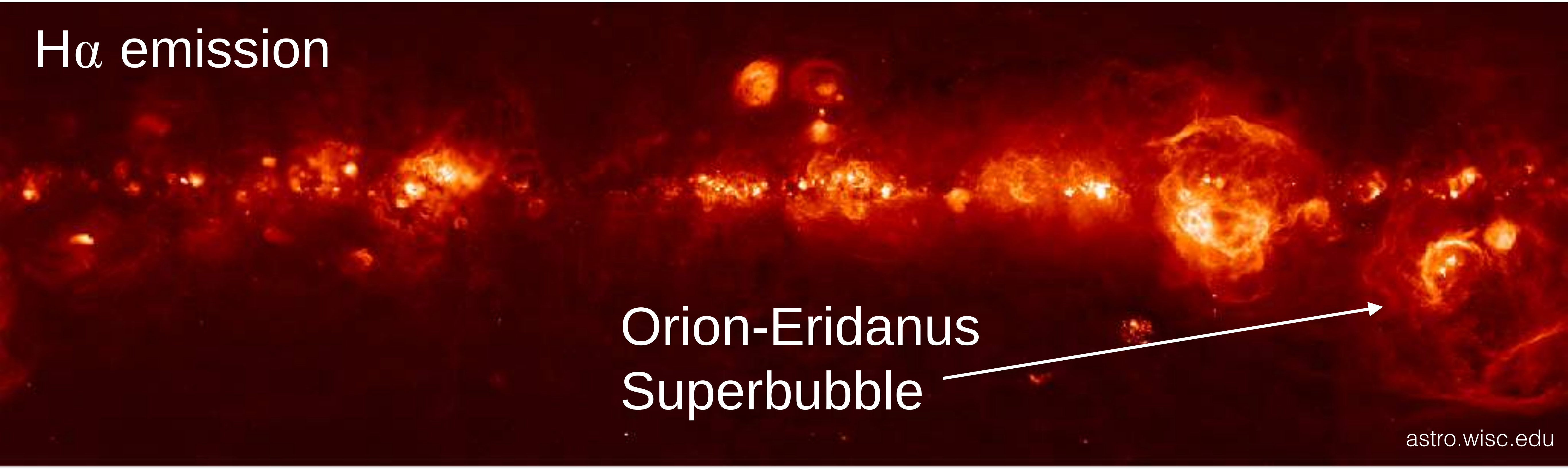

Stellar Winds (SW) and SNe Effects on ISM

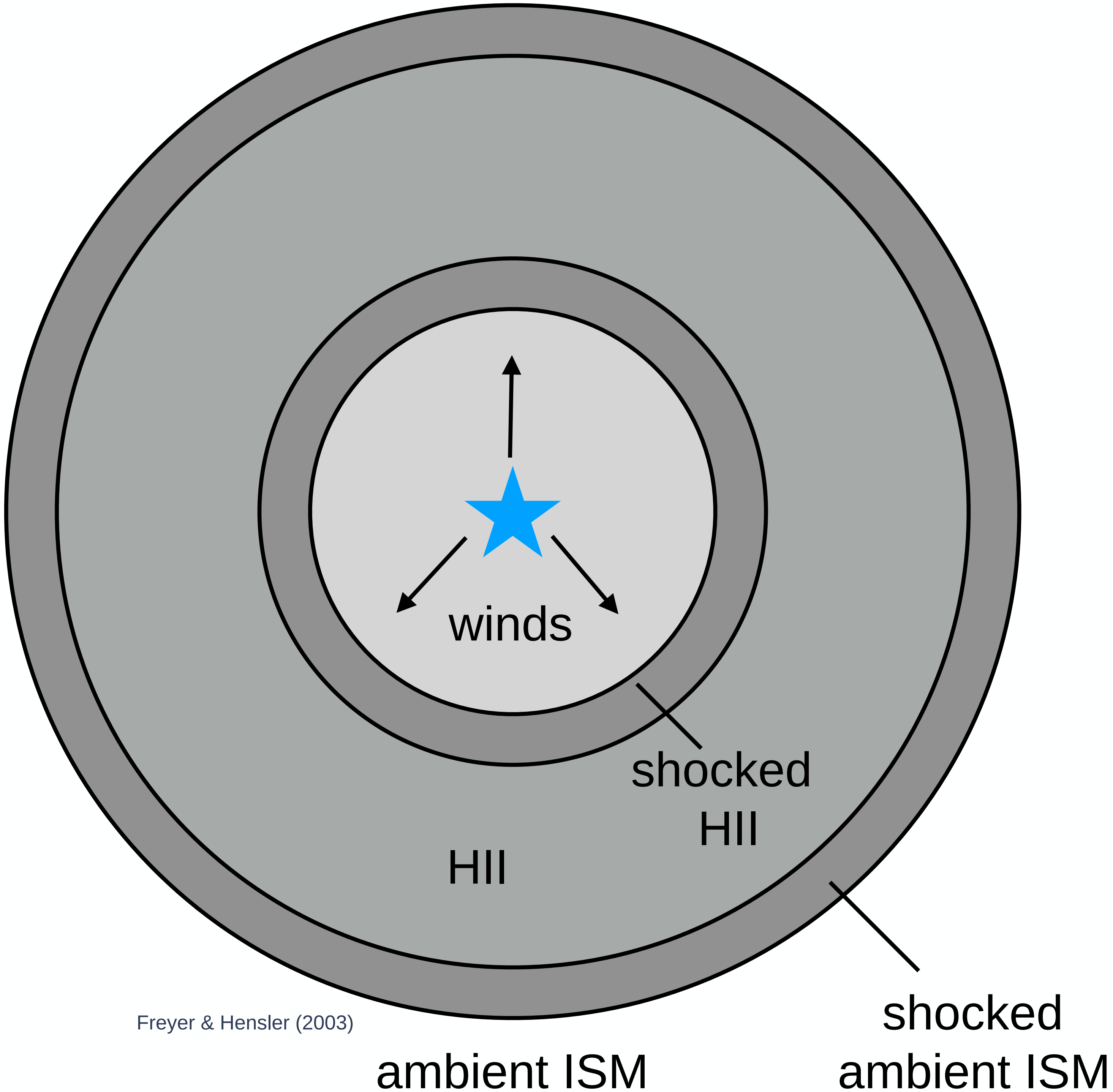

Freyer & Hensler (2003)

SW and SNe Effects on Magnetic Fields

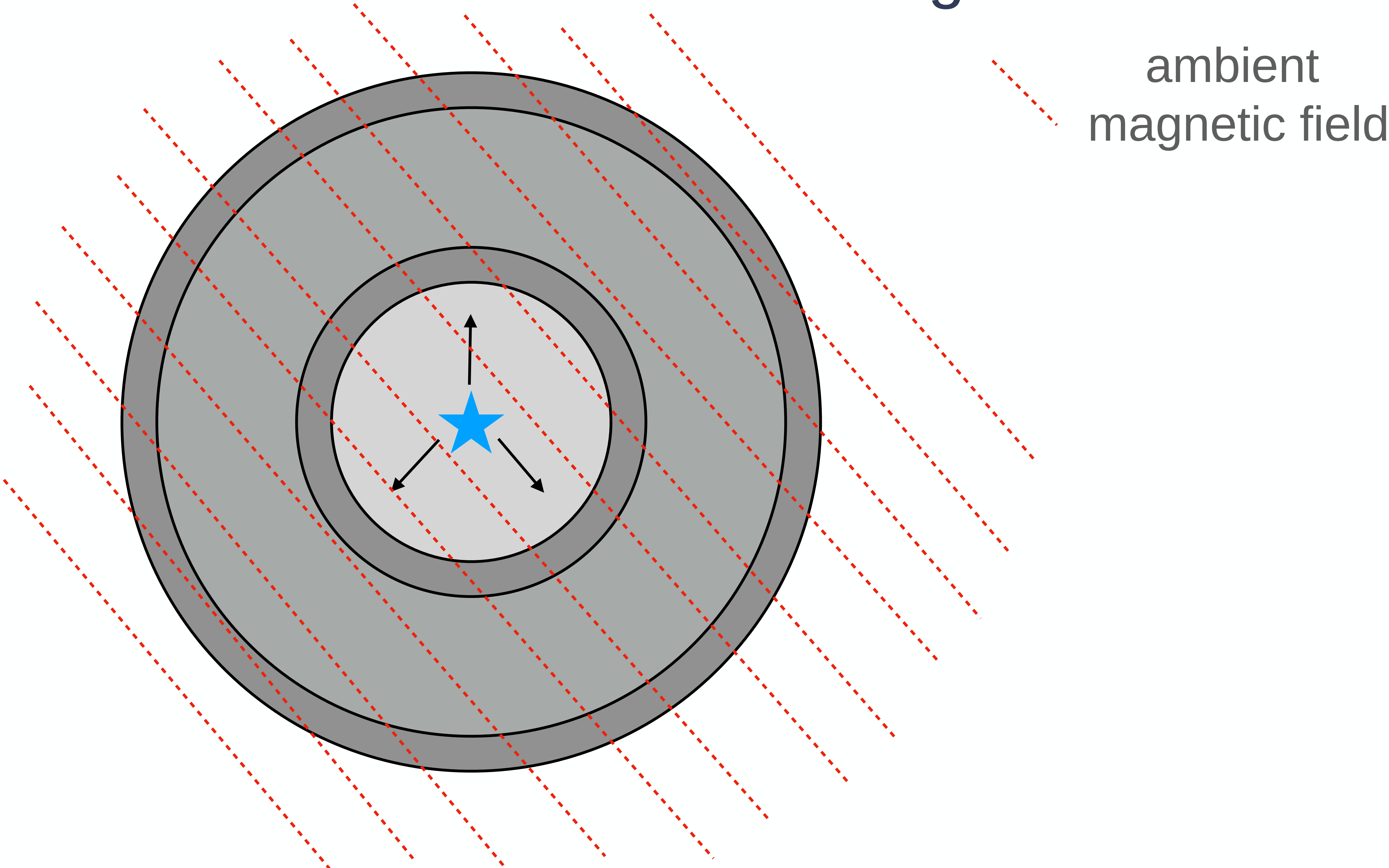

SW and SNe Effects on Magnetic Fields

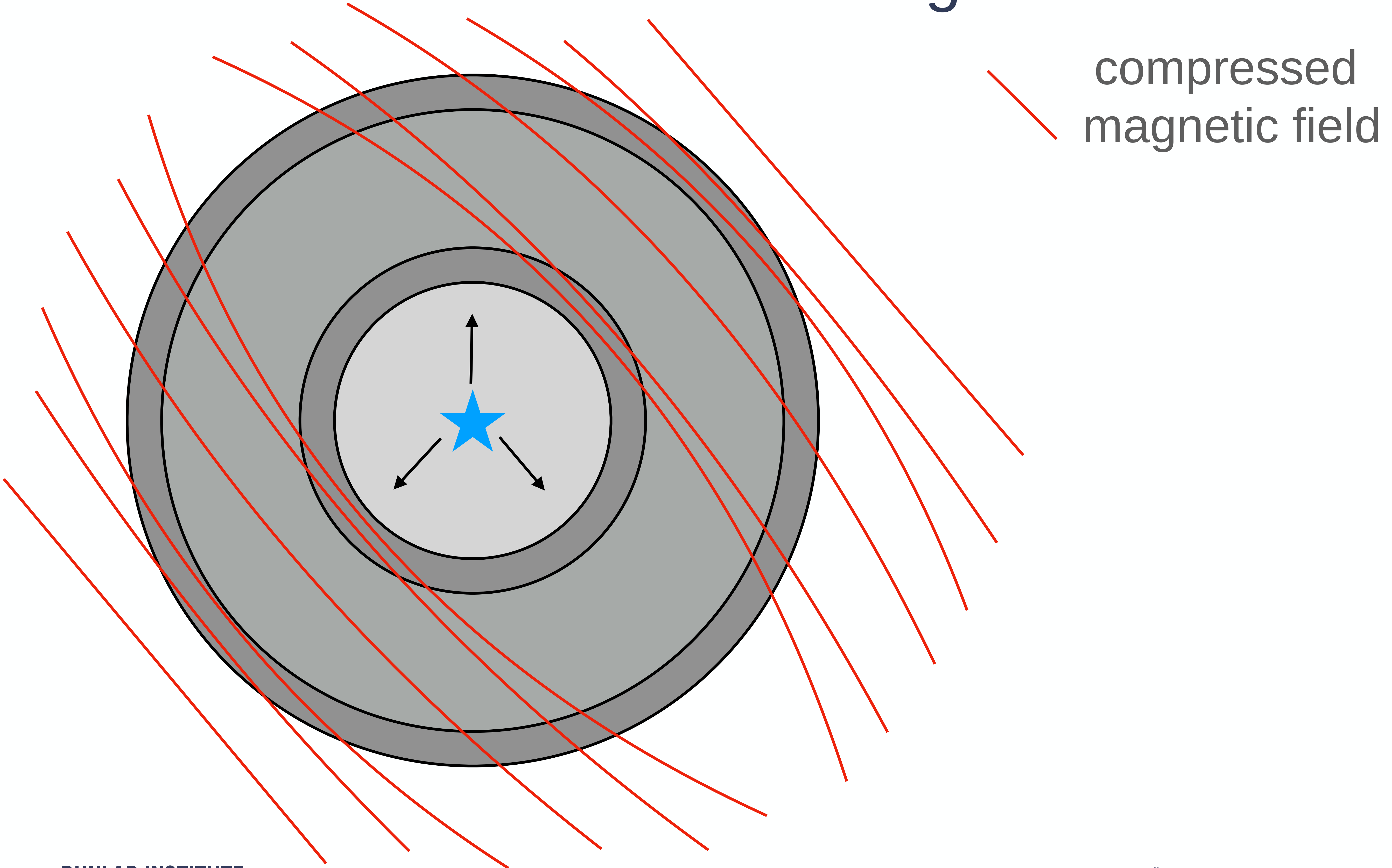

Determining Origin of Loops and Superbubbles

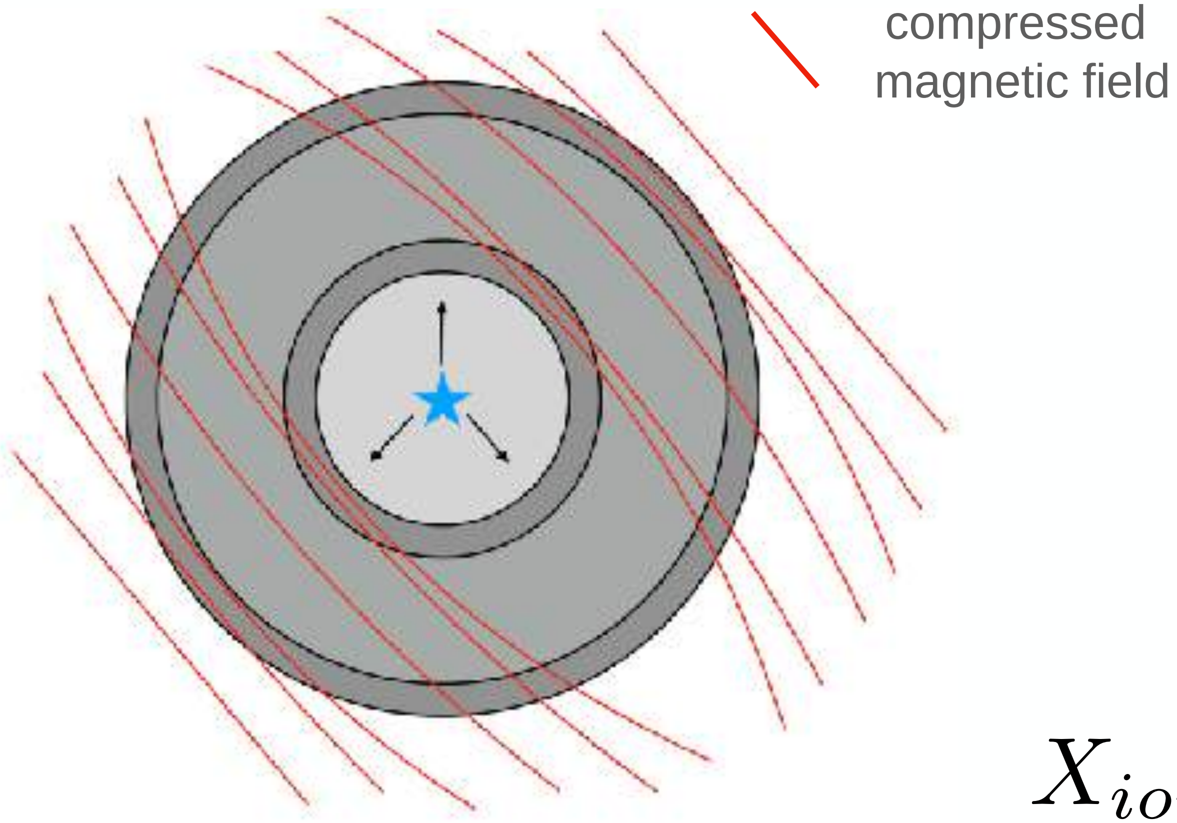

compression factor:

$$X_B = \frac{B}{B_0}$$

object's magnetic field

ambient magnetic field

ionization fraction:

$$X_{ion} = \frac{n_{H^+}}{n_{H^+} + n_H}$$

plasma number density

total number density

(1) Young SNe and windblown bubbles: $X_B \lesssim 4$

(2) Old SNe (time to cool): $X_B \approx 100$

(3) Ionization fronts and HII regions: $X_B \approx 1$

Magnetic Field Strengths

Faraday rotation:

$$\chi = \chi_0 + (\mathrm{RM})\lambda^2$$

$$\mathrm{RM} = 0.81 \int_{\mathrm{source}}^{\mathrm{observer}} n_e \vec{B} \cdot \vec{dl}$$

χ polarization angle
RM rotation measure
λ observation wavelength
n_e thermal electron density

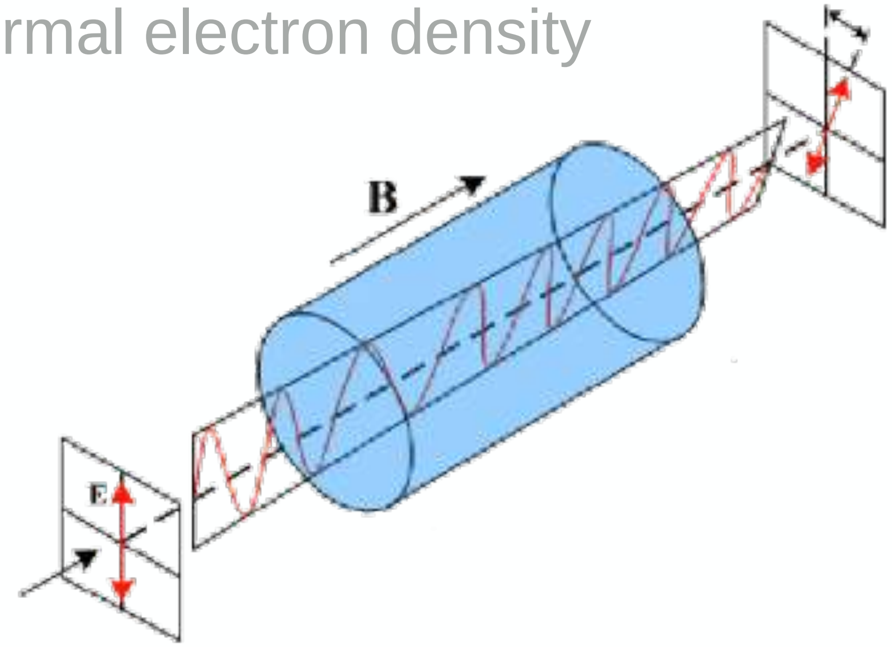

Magnetic Field Strengths

Faraday rotation:

$$\chi = \chi_0 + (\mathrm{RM})\lambda^2$$

$$\mathrm{RM} = 0.81 \int_{\mathrm{source}}^{\mathrm{observer}} n_e \vec{B} \cdot \vec{dl}$$

χ polarization angle
RM rotation measure
λ observation wavelength
n_e thermal electron density

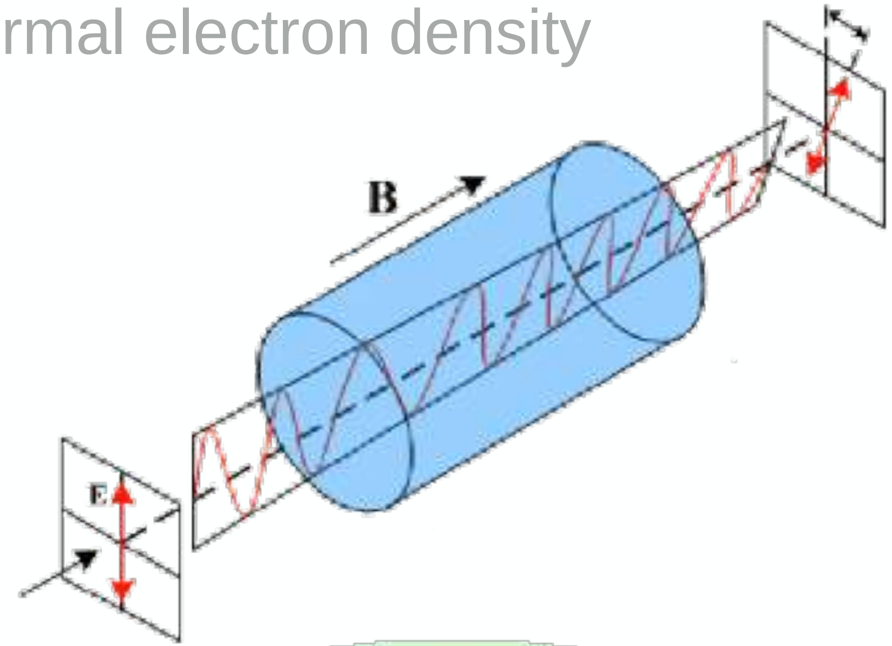

Assuming spherical shell geometry:

$$\left(\frac{\mathrm{RM}}{\mathrm{rad\,m^{-2}}}\right) = 0.81 \left(\frac{n_e}{\mathrm{cm^{-3}}}\right) \left(\frac{B_{\parallel}}{\mu G}\right) f_{\mathrm{ion}} \left(\frac{L}{\mathrm{pc}}\right)$$

f_{ion} plasma filling factor
L path length
$(f_{\mathrm{ion}} L)$ occupation length

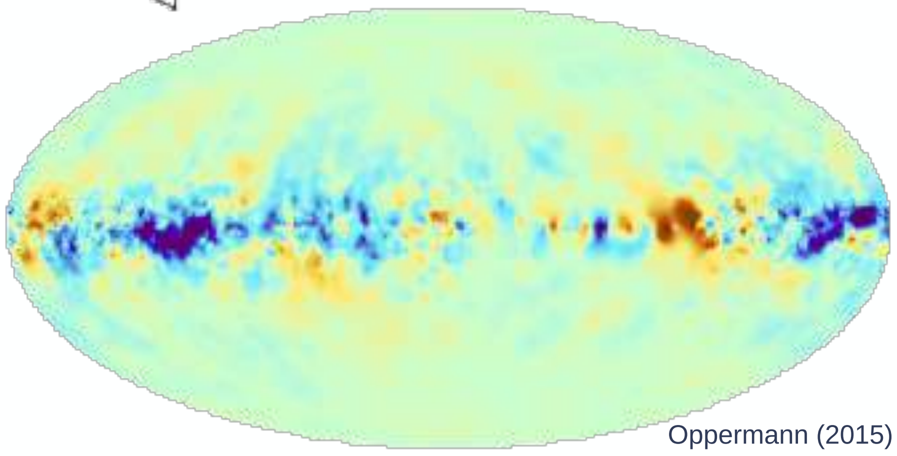

Oppermann (2015)

Magnetic Field Strengths

Faraday rotation:

$$\chi = \chi_0 + (\mathrm{RM})\lambda^2$$

$$\mathrm{RM} = 0.81 \int_{\mathrm{source}}^{\mathrm{observer}} n_e \vec{B} \cdot d\vec{l}$$

χ polarization angle

RM rotation measure

λ observation wavelength

n_e thermal electron density

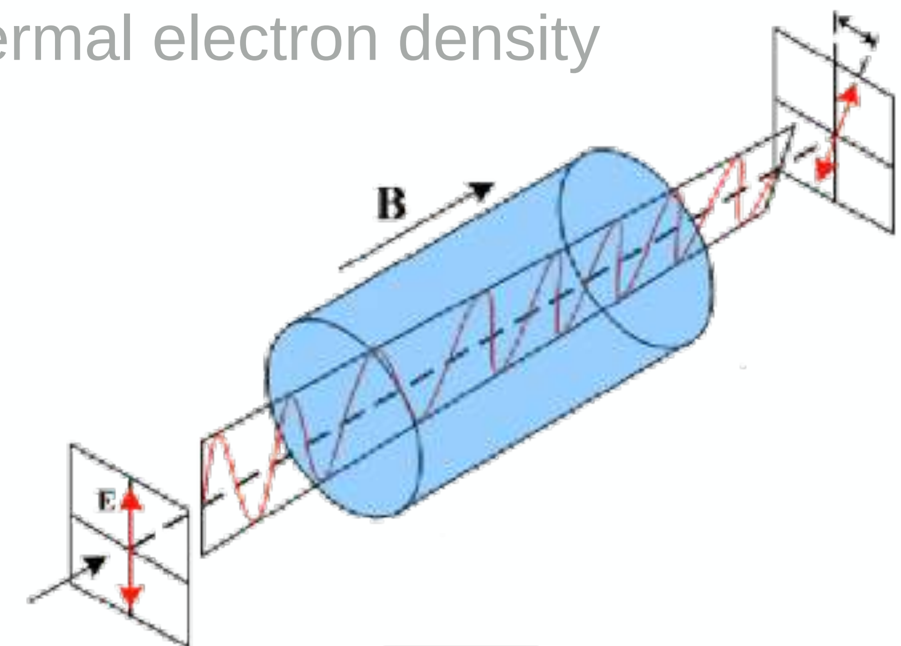

Assuming spherical shell geometry:

$$\left(\frac{\mathrm{RM}}{\mathrm{rad\,m^{-2}}}\right) = 0.81 \left(\frac{n_e}{\mathrm{cm^{-3}}}\right) \left(\frac{B_{\parallel}}{\mu G}\right) f_{\mathrm{ion}} \left(\frac{L}{\mathrm{pc}}\right)$$

f_{ion} plasma filling factor

L path length

$(f_{\mathrm{ion}} L)$ occupation length

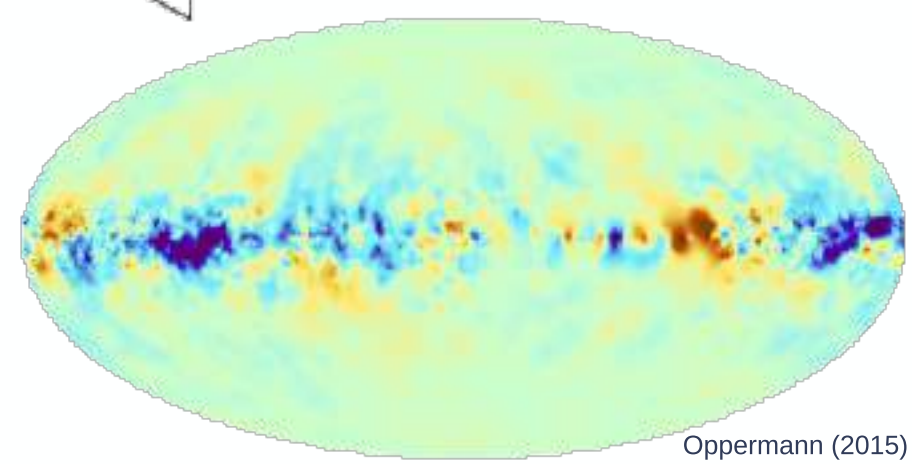

Oppermann (2015)

Thermal Electron Densities

H-α emission measure:

$$\mathrm{EM} = \int_0^\infty n_e^2 dl$$

$$\left(\frac{\mathrm{EM}}{\mathrm{pc\,cm^{-6}}}\right) = 9.41 \times 10^8 \left(\frac{T_e}{10^4\,\mathrm{K}}\right)^{1.134}$$

$$\times 10^{0.038\left(\frac{10^4\,\mathrm{K}}{T_e}\right)} \left(\frac{I(H\alpha)}{\mathrm{erg\,cm^{-2}\,s^{-1}\,sr^{-1}}}\right)$$

Wisconsin Hα Mapper (WHAM) Survey

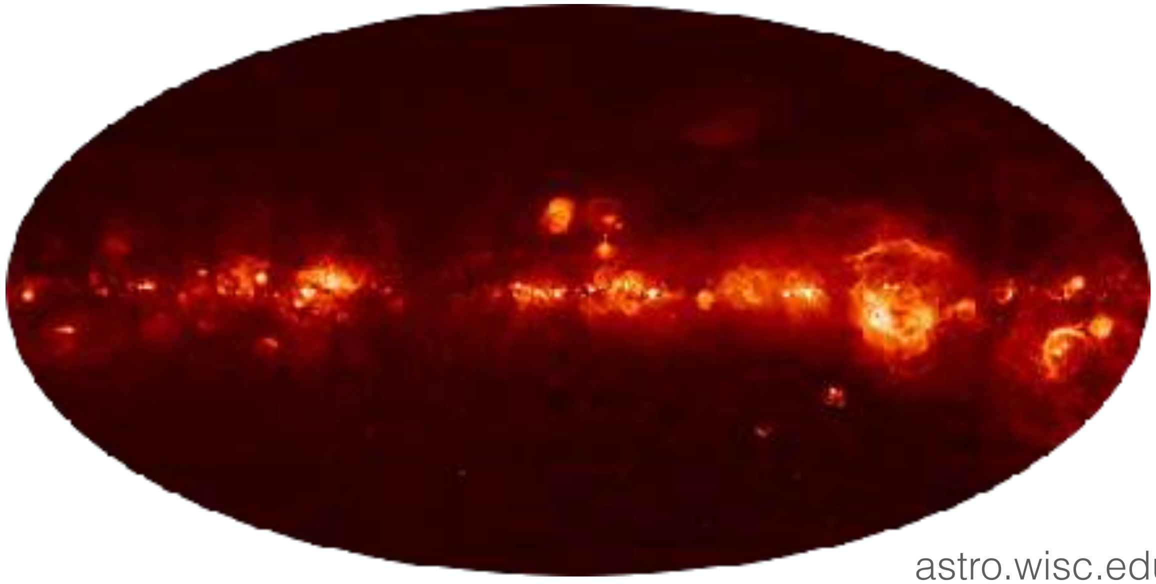

astro.wisc.edu

Thermal Electron Densities

H-α emission measure:

Wisconsin Hα Mapper (WHAM) Survey

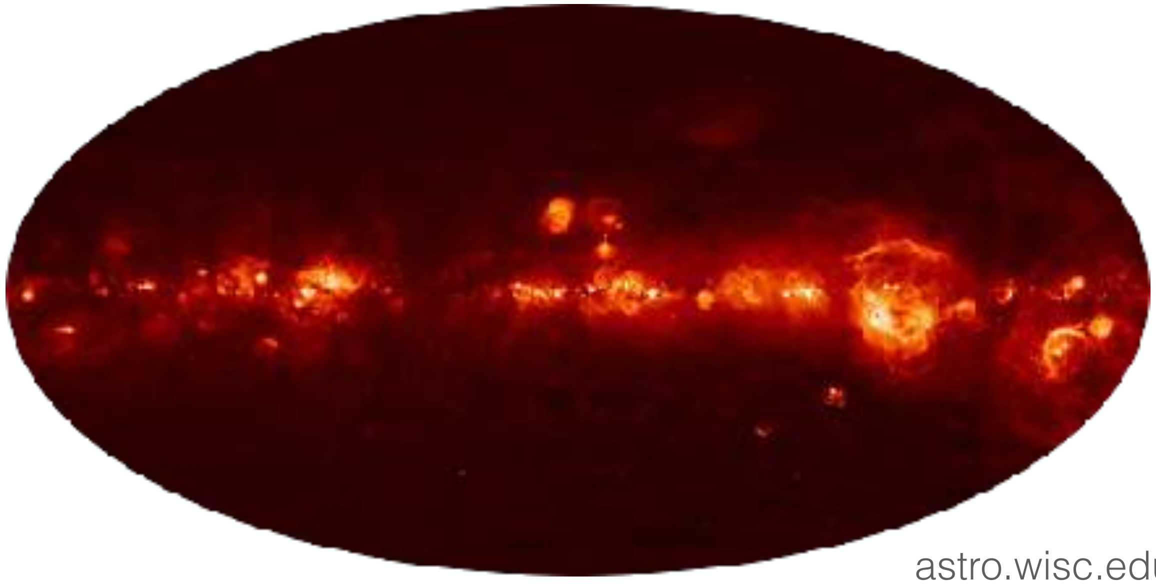

astro.wisc.edu

$$\mathrm{EM} = \int_0^\infty n_e^2 dl$$

$$\left(\frac{\mathrm{EM}}{\mathrm{pc\,cm^{-6}}}\right) = 9.41 \times 10^8 \left(\frac{T_e}{10^4\,\mathrm{K}}\right)^{1.134} \times 10^{0.038\left(\frac{10^4\,\mathrm{K}}{T_e}\right)} \left(\frac{I(H\alpha)}{\mathrm{erg\,cm^{-2}\,s^{-1}\,sr^{-1}}}\right)$$

Assuming spherical shell geometry:

$$\left(\frac{\mathrm{EM}}{\mathrm{pc\,cm^{-6}}}\right) = \left(\frac{n_e}{\mathrm{cm^{-3}}}\right)^2 f_{\mathrm{ion}} \left(\frac{L}{\mathrm{pc}}\right)$$

f_{ion} plasma filling factor

L path length

$(f_{\mathrm{ion}} L)$ occupation length

Neutral Atomic HI Number Density

HI4PI Survey

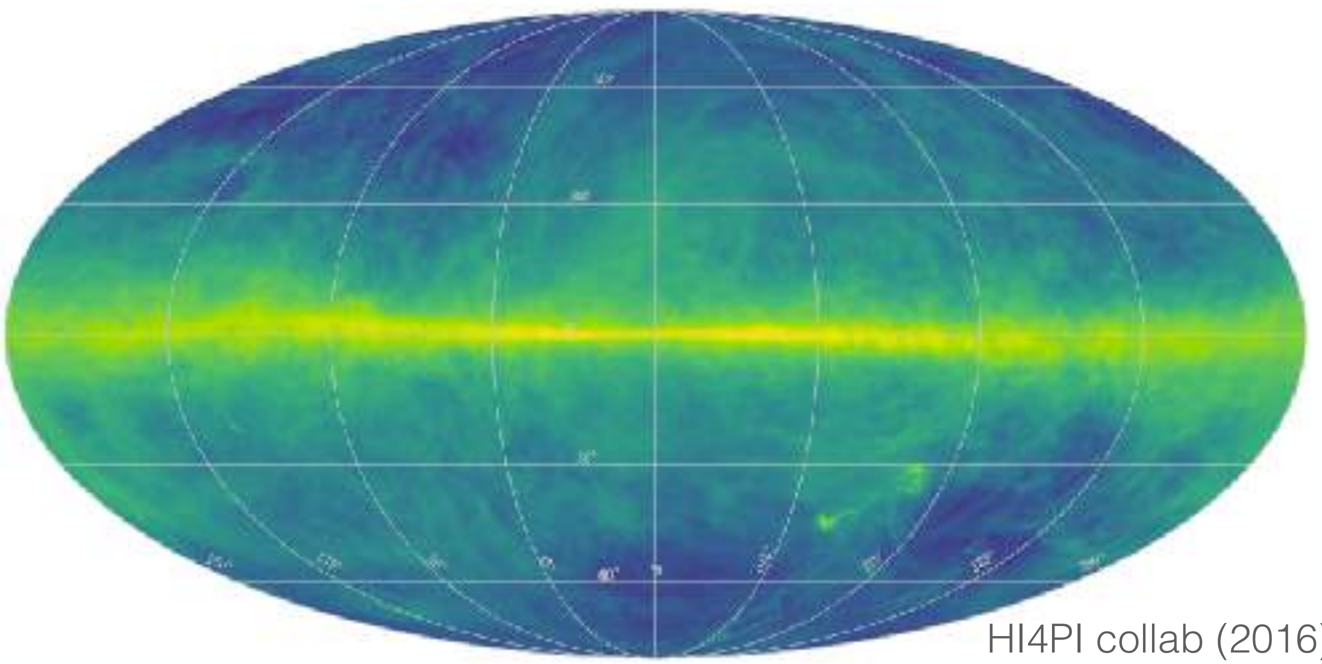

HI4PI collab (2016)

21-cm HI column density:

$$N(\mathrm{HI}) = \int_0^\infty n(\mathrm{HI})\, ds$$

Assuming spherical shell geometry:

$$\left(\frac{N(\mathrm{HI})}{\mathrm{cm}^{-2}}\right) = \left(\frac{n(\mathrm{HI})}{\mathrm{cm}^{-3}}\right) f_{\mathrm{neut}} \left(\frac{L}{\mathrm{pc}}\right)$$

f_{neut} neutral filling factor

L path length

$(f_{\mathrm{neut}} L)$ occupation length

$$f_{\mathrm{ion}} + f_{\mathrm{neut}} = 1$$

Loop III and the Intermediate Velocity (IV) Arch

408 MHz synchrotron

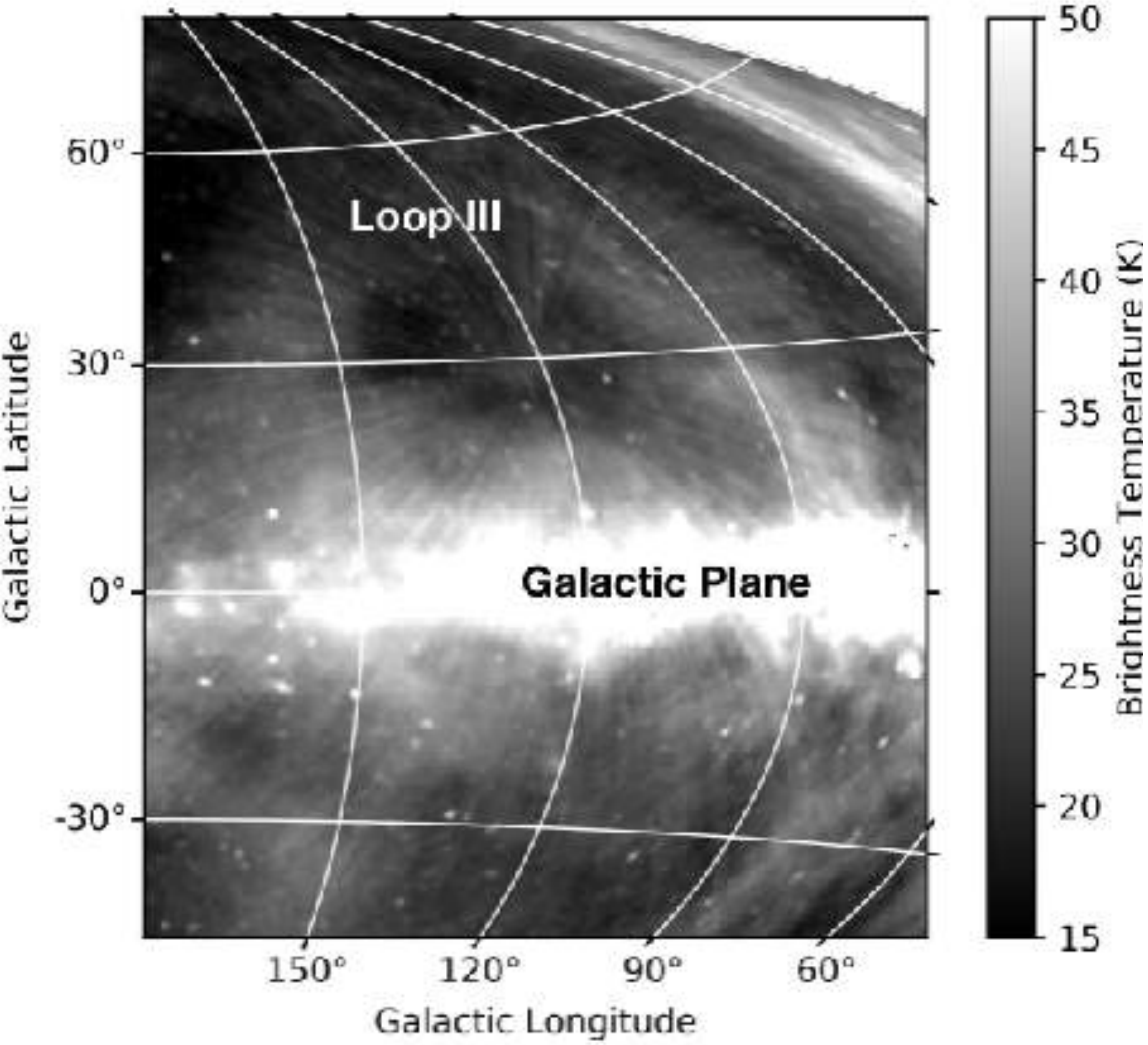

HI4PI HI

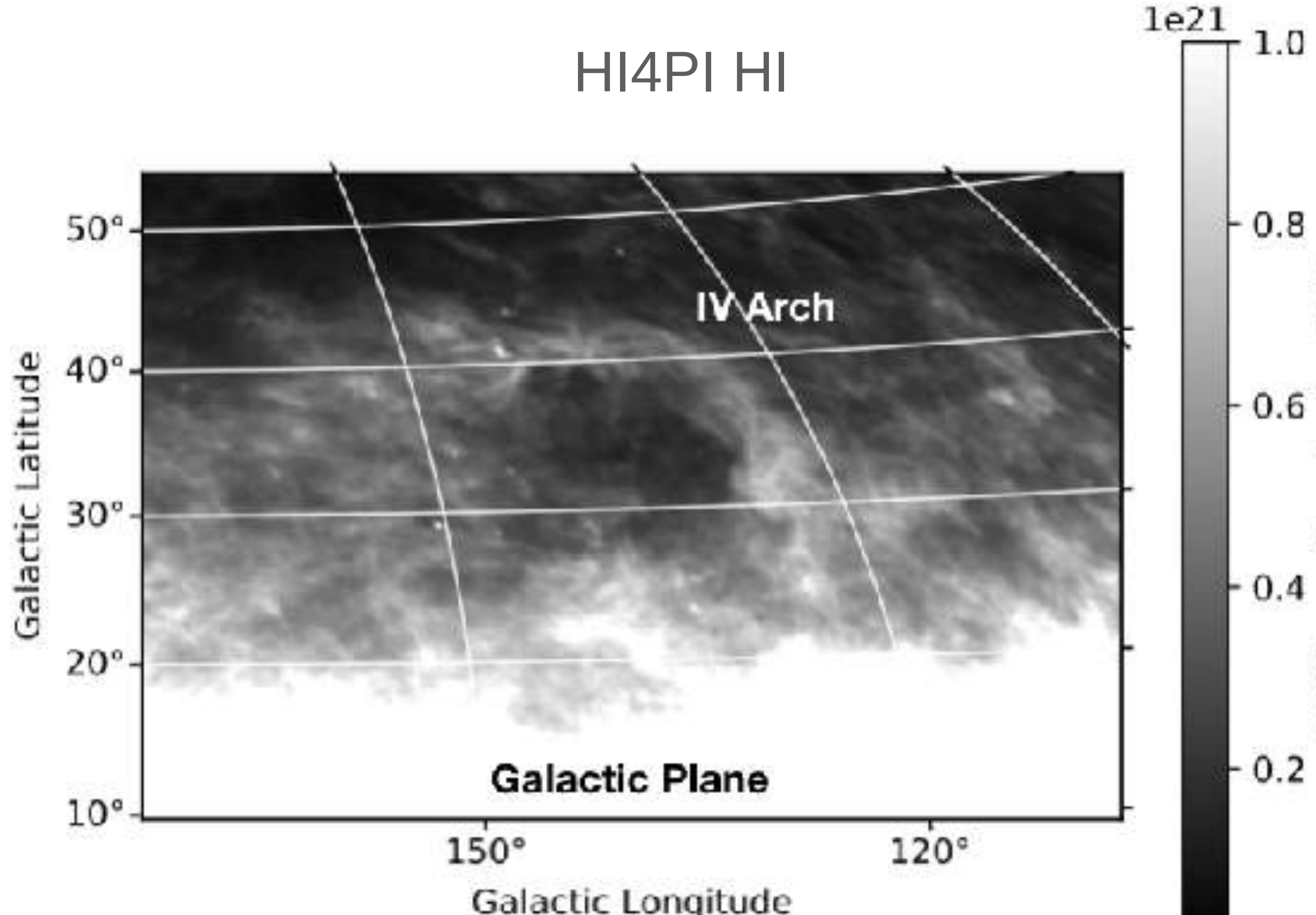

Orion-Eridanus Superbubble and Barnard's Loop

WHAM Hα

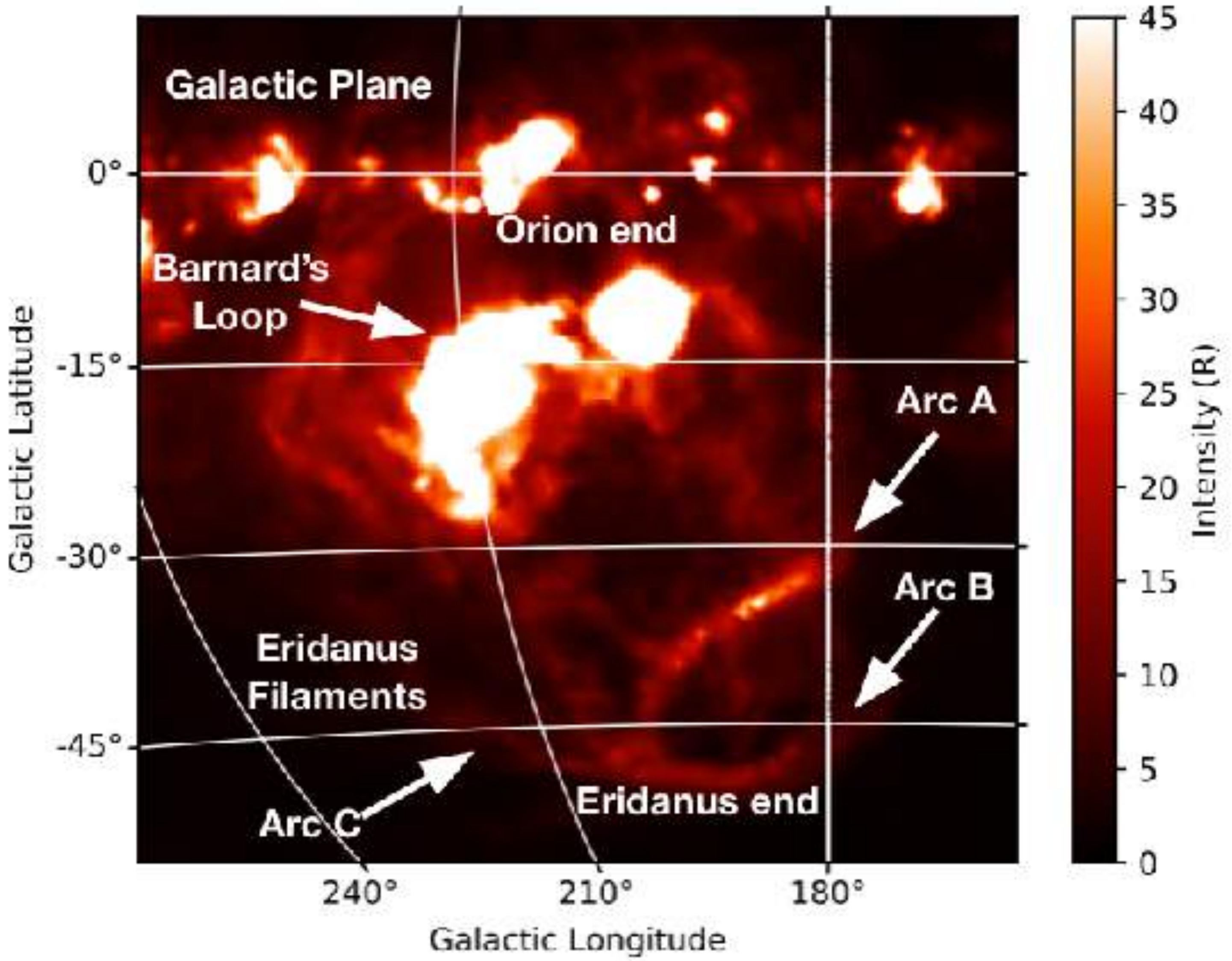

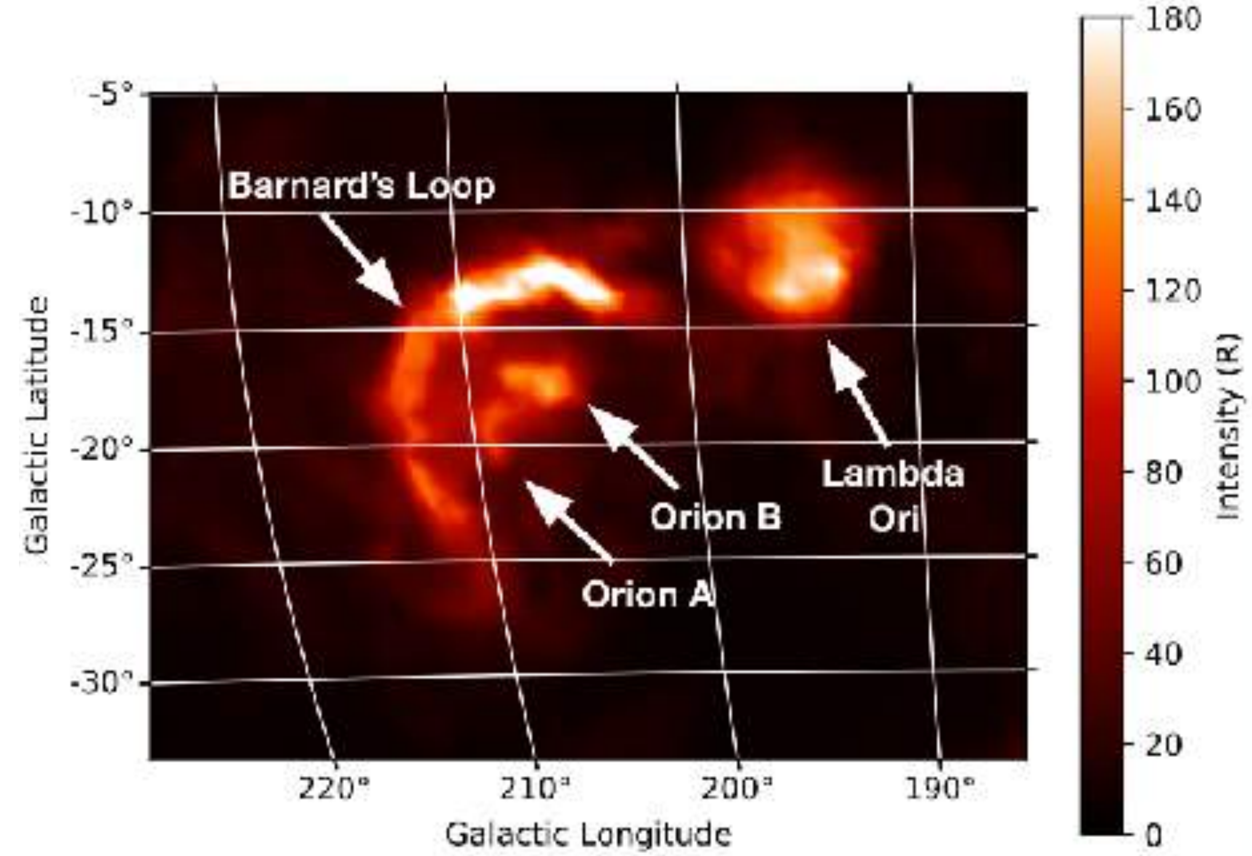

Loops in Rotation Measure

Loop III:

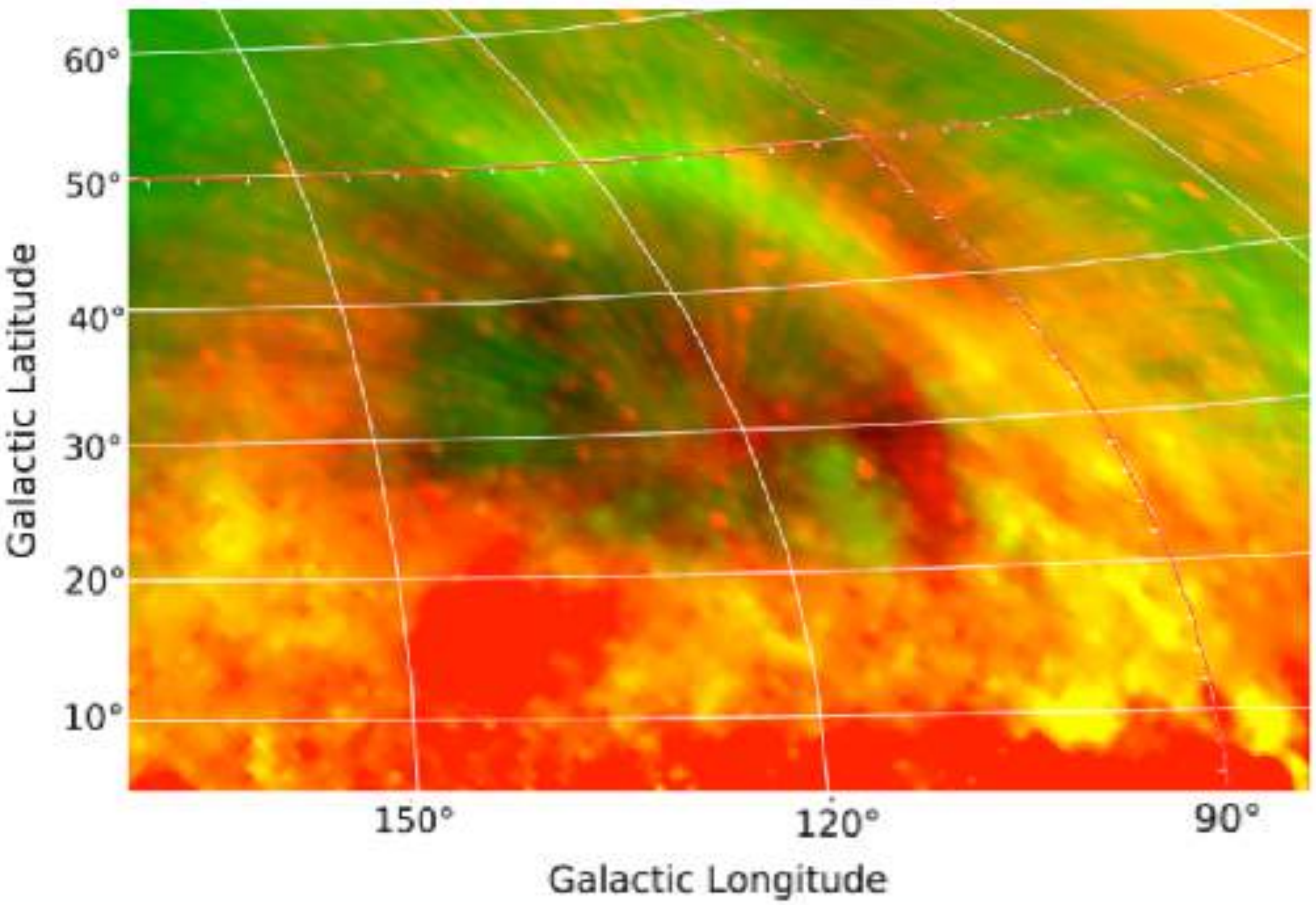

Green: **RM = -15 rad m^{-2}**
Red: 408 MHz synchrotron

Intermediate Velocity (IV) Arch:

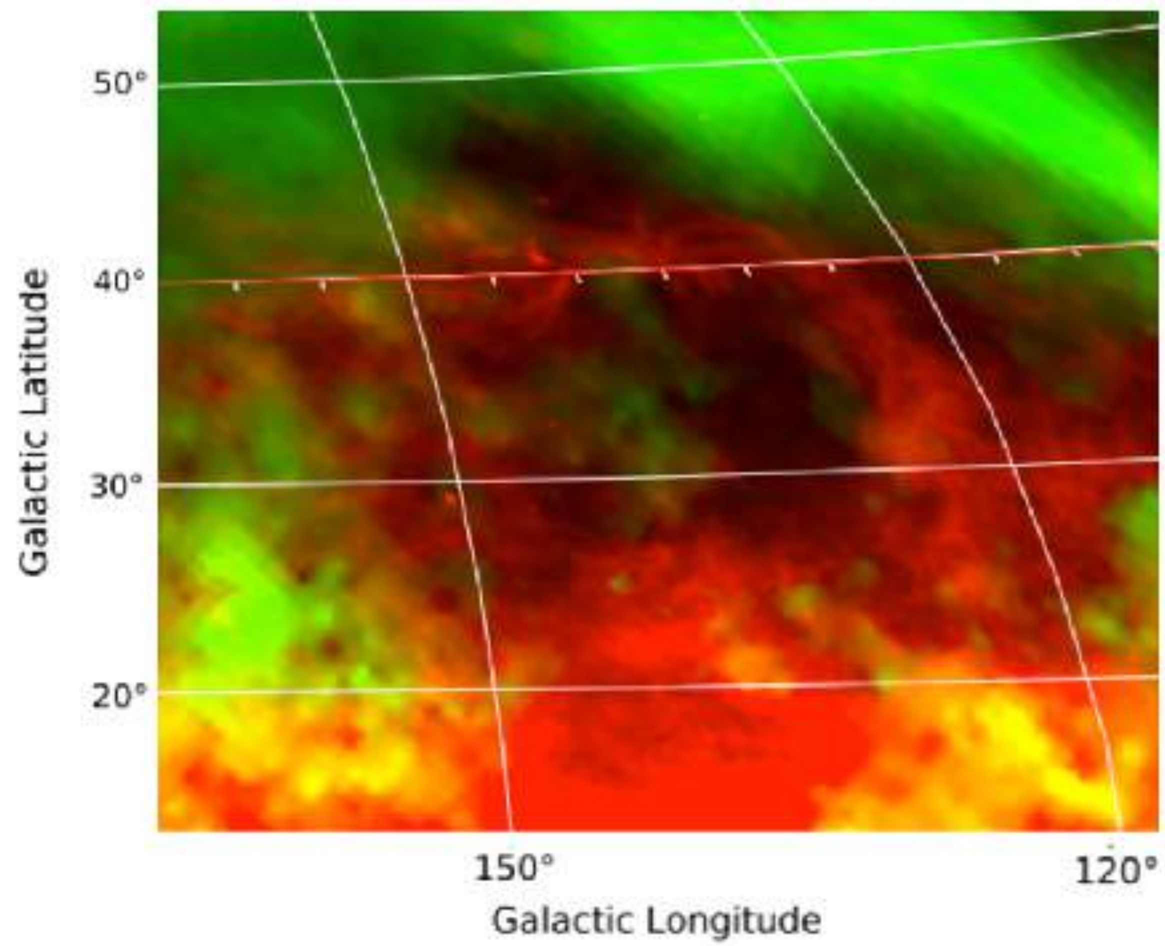

Green: **RM = -5 rad m^{-2}**
Red: HI4PI neutral HI

Loops in Rotation Measure

Loop III:

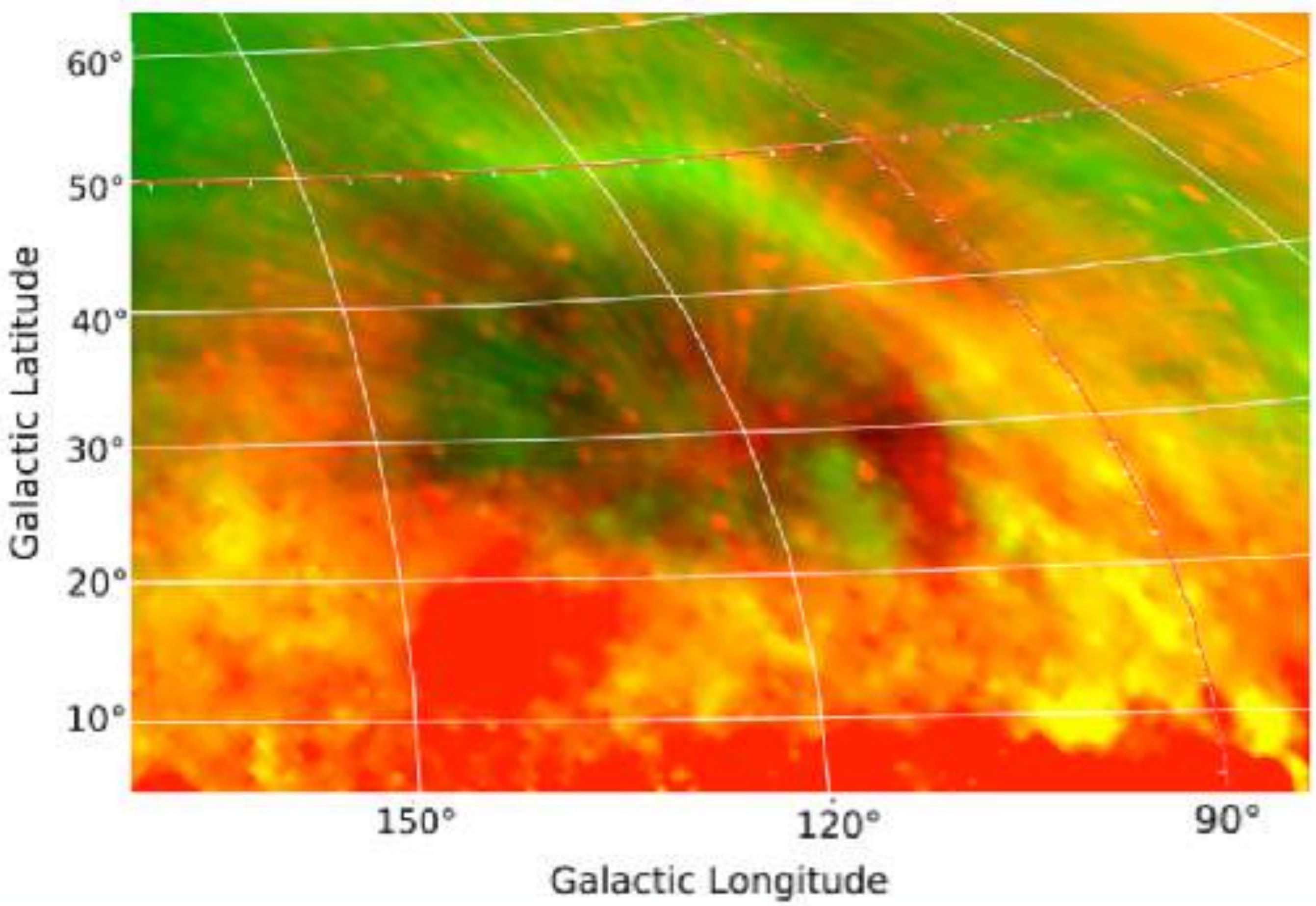

Green: **RM = -15 rad m^{-2}**
Red: 408 MHz synchrotron

$$|B_{||}| \lesssim 1.83 - 5.1\,\mu G$$

$$X_B = 1.6 - 3.2$$

Intermediate Velocity (IV) Arch:

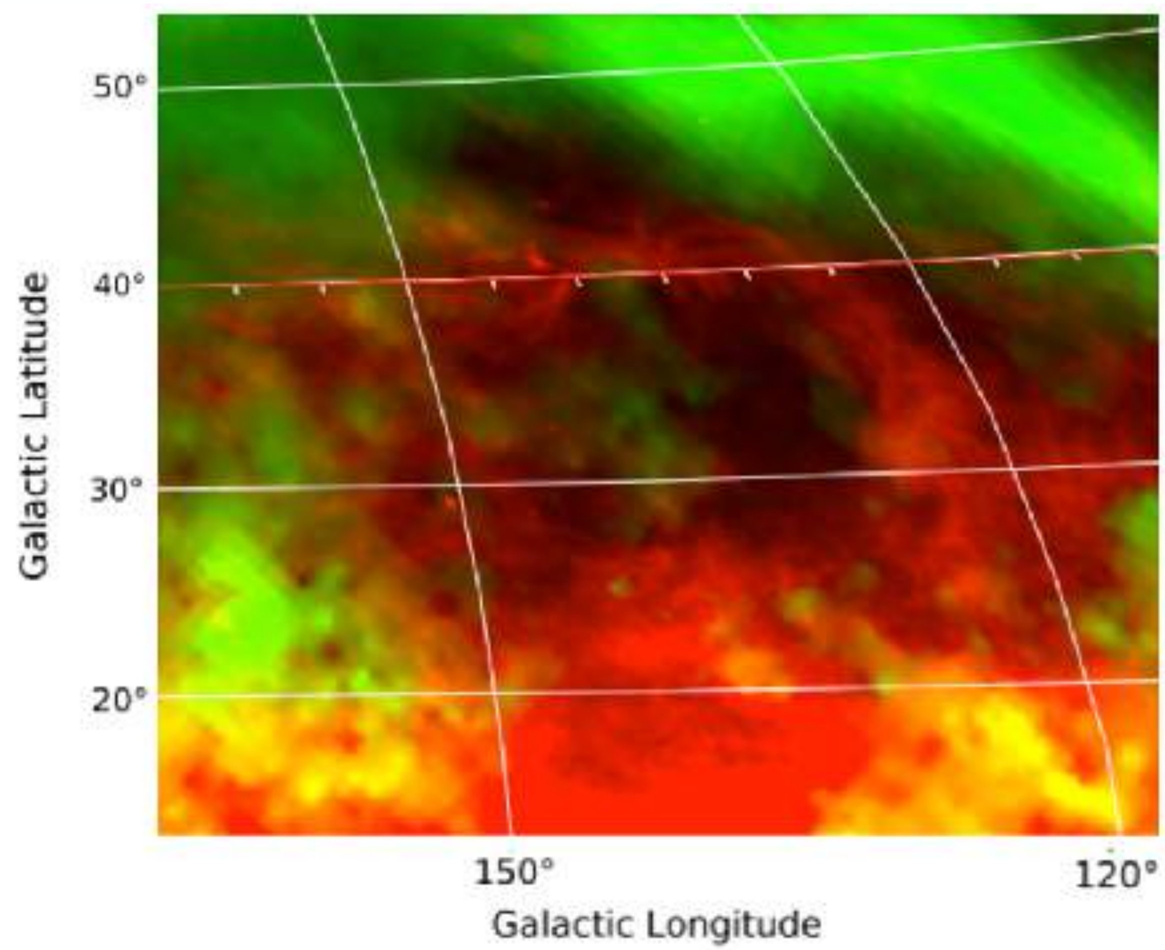

Green: **RM = -5 rad m^{-2}**
Red: HI4PI neutral HI

$$|B_{||}| = 1.7 - 4.7 \mu G$$

$$X_B \lesssim 1 - 3$$

Superbubble in Rotation Measure

Orion-Eridanus Superbubble

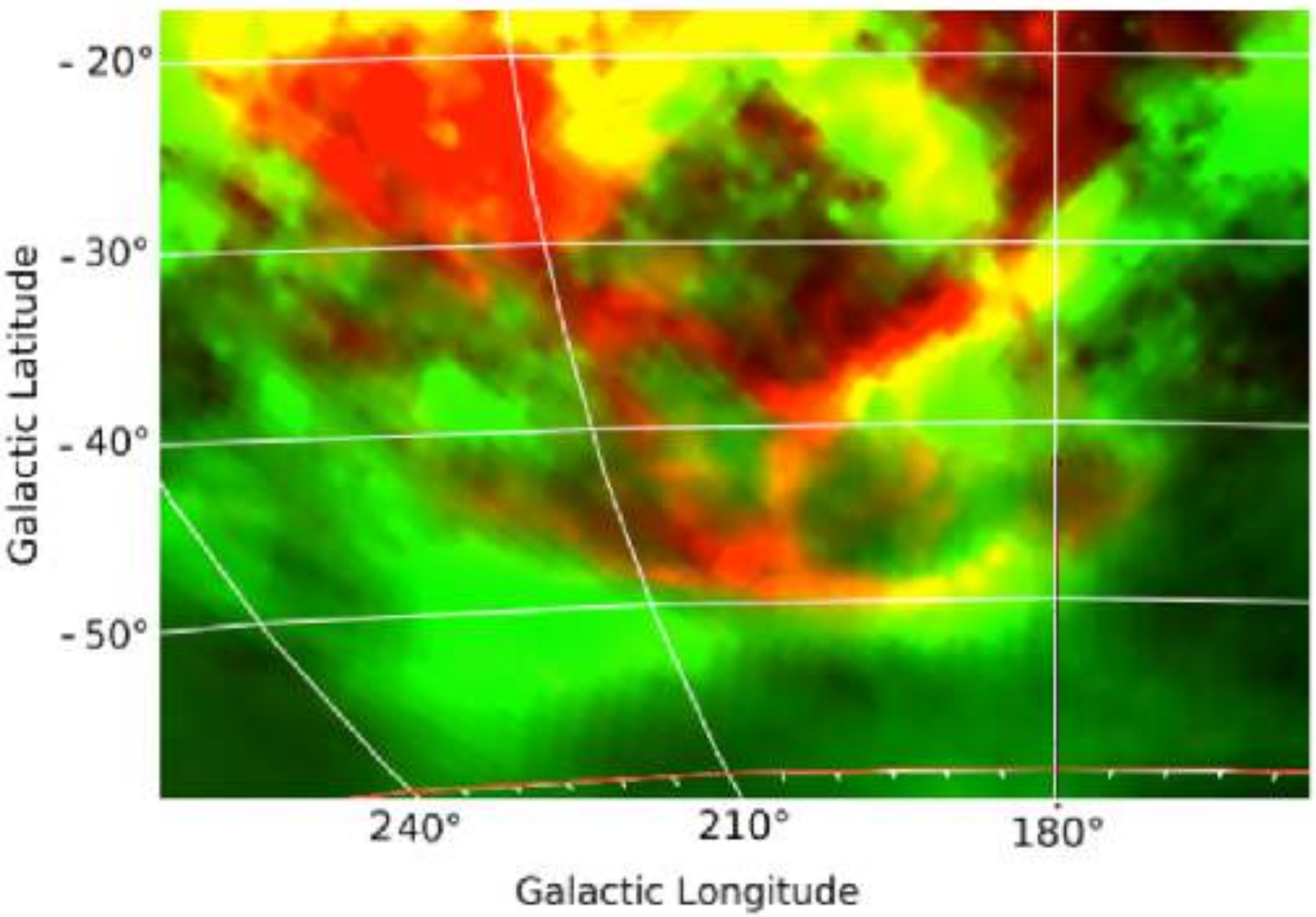

Green: **RM = 10 rad m^{-2}**
Red: WHAM Hα

Barnard's Loop

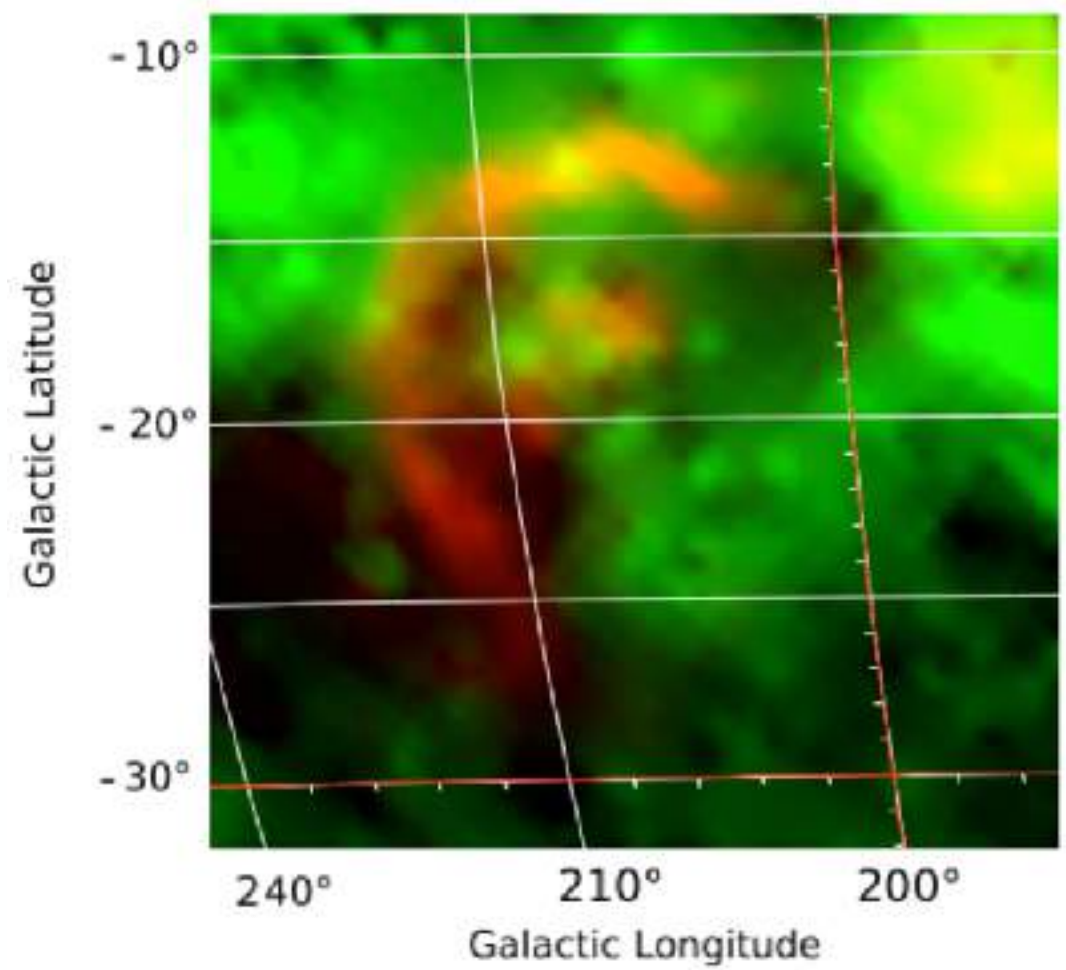

Green: **RM = 40 rad m^{-2}**
Red: WHAM Hα

Superbubble in Rotation Measure

Orion-Eridanus Superbubble

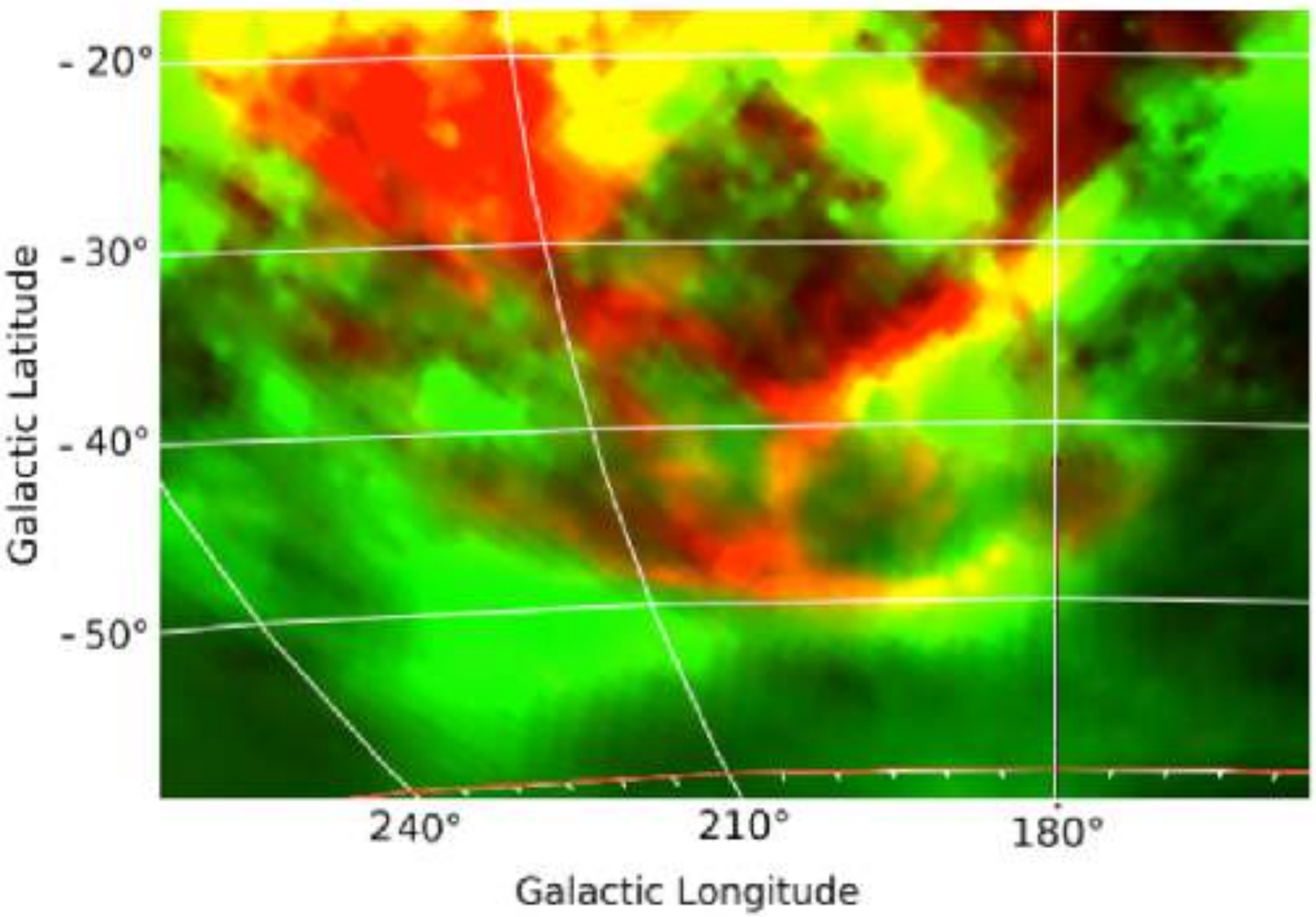

Green: **RM = 10 rad m^{-2}**

Red: WHAM Hα

$$B_{\|} = 2.4\,\mu G$$
$$X_B = 1.5$$

Barnard's Loop

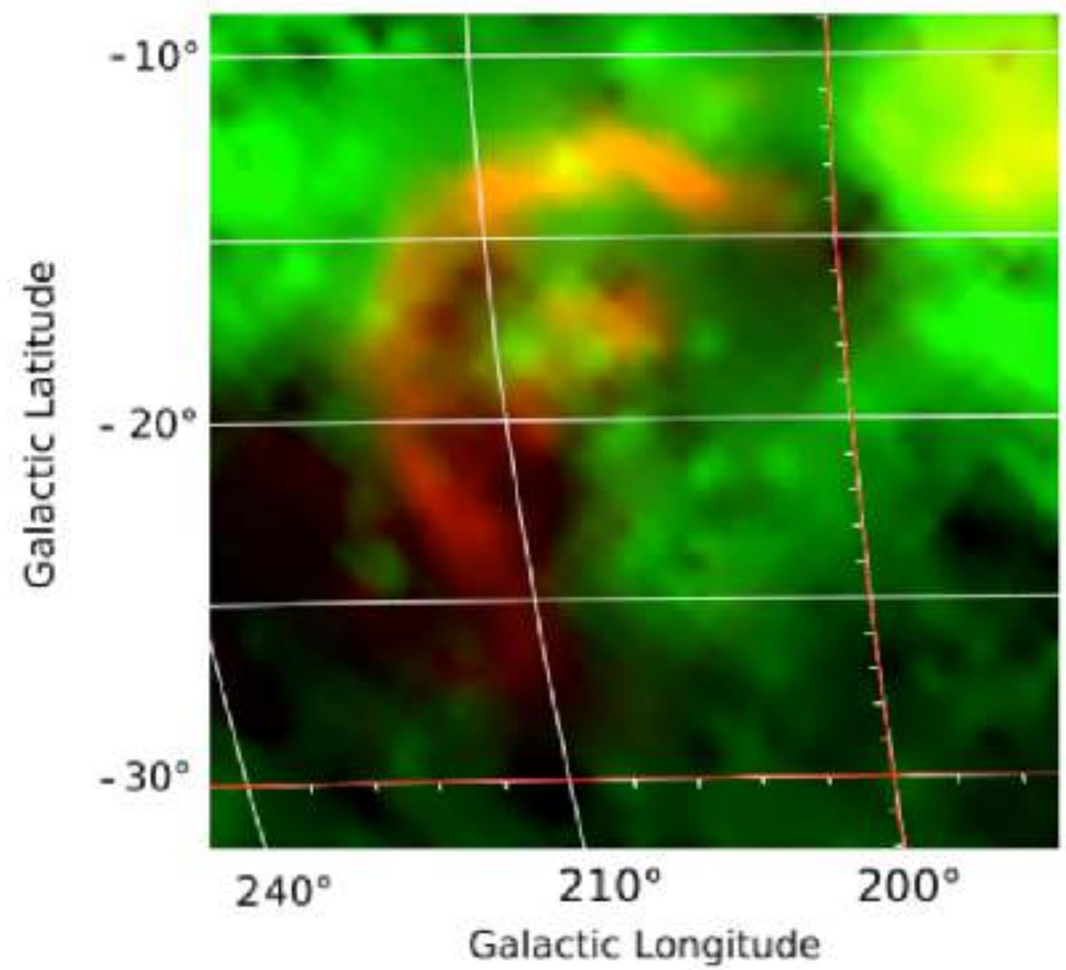

Green: **RM = 40 rad m^{-2}**

Red: WHAM Hα

$$B_{\|} = 3.5\,\mu G$$
$$X_B = 2.2$$

Orion-Eridanus Superbubble in Depolarization

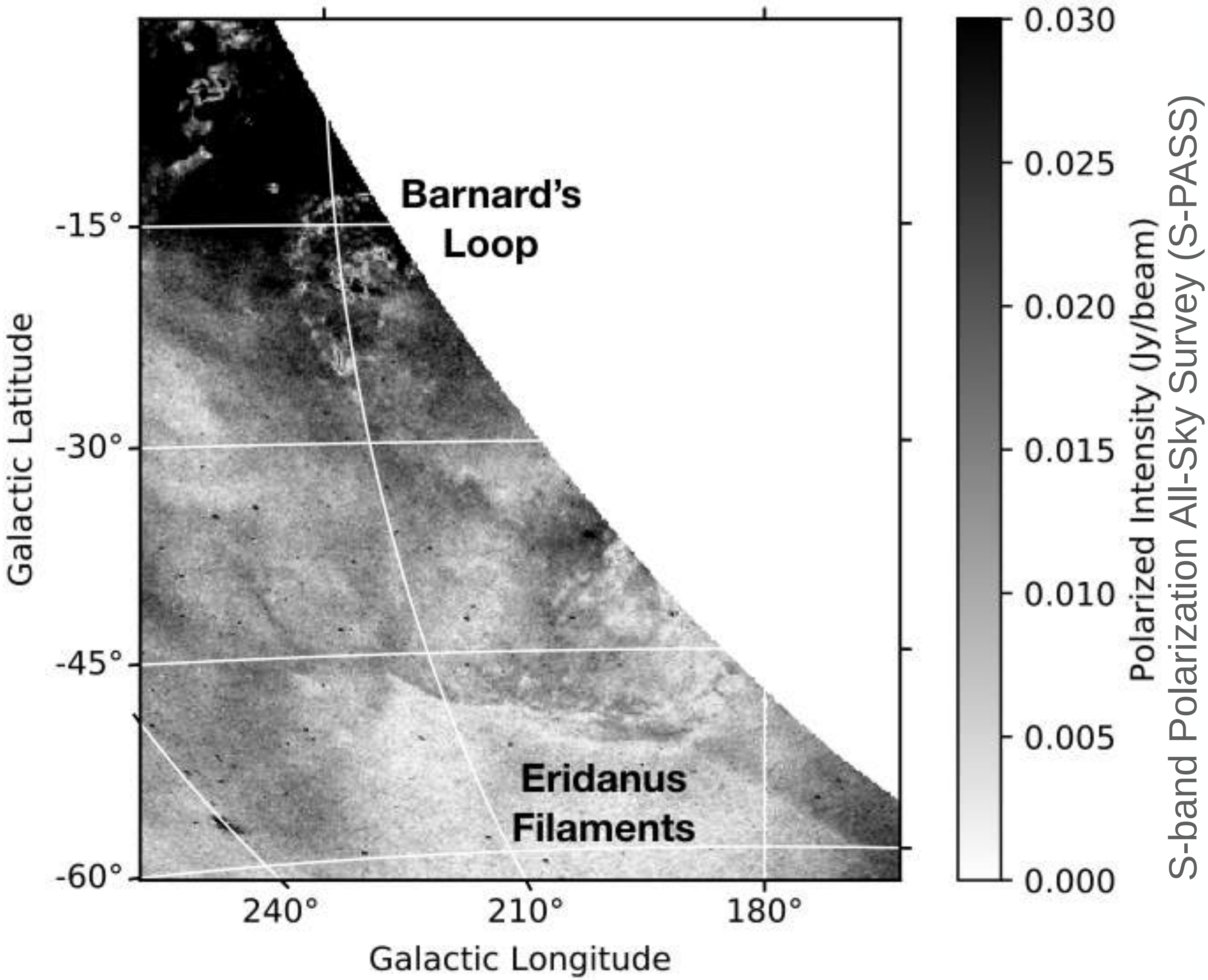

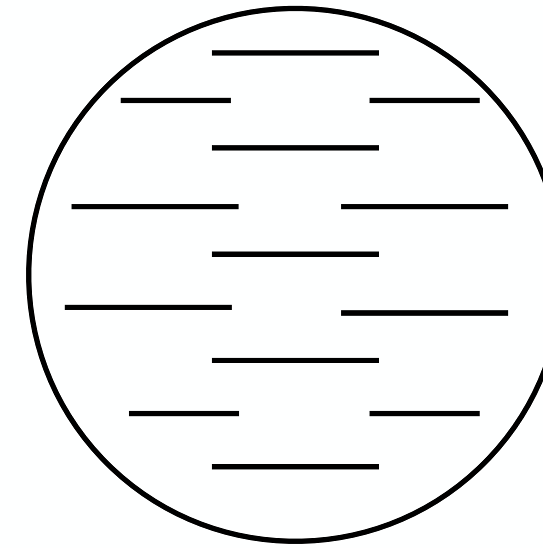

p(5/3) ~ 67%

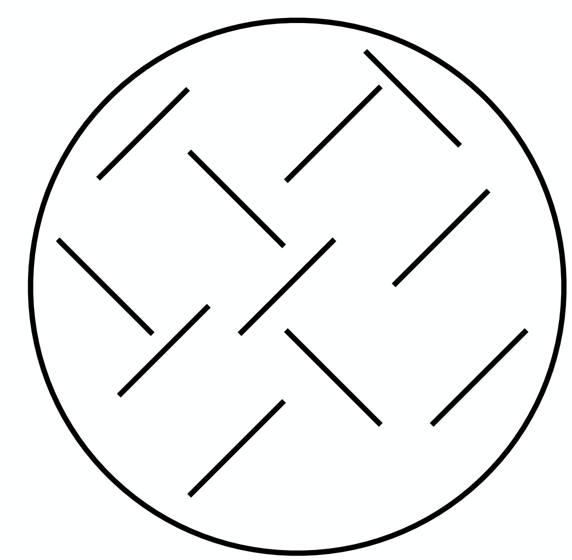

p(5/3) < 67%

Summary

- Radio Loops and Superbubbles are among the largest features in the Galaxy whose origin remains unclear
- Compression factor of magnetic field can help differentiate between various models of origin along with ionization
- Loop III is possibly the result of stellar winds emanating from massive stars in the Galactic plane
- The Orion-Eridanus Superbubble filaments may have been pre-existing density structures ionized from stars in Orion
- Barnard's Loop might have been an ionization front triggered by the massive stars in Orion
- Orion-Eridanus Superbubble Filaments and the outer region of Barnard's Loop seen in beam depolarization; indication of a turbulent magnetic field

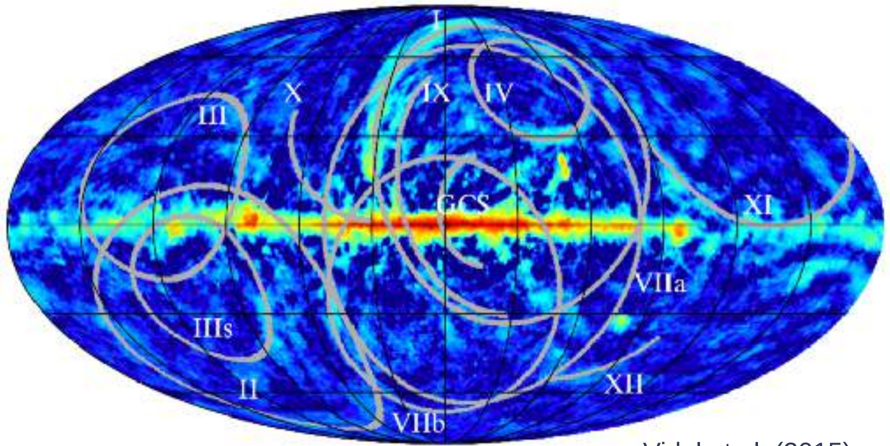

Vidal et al. (2015)

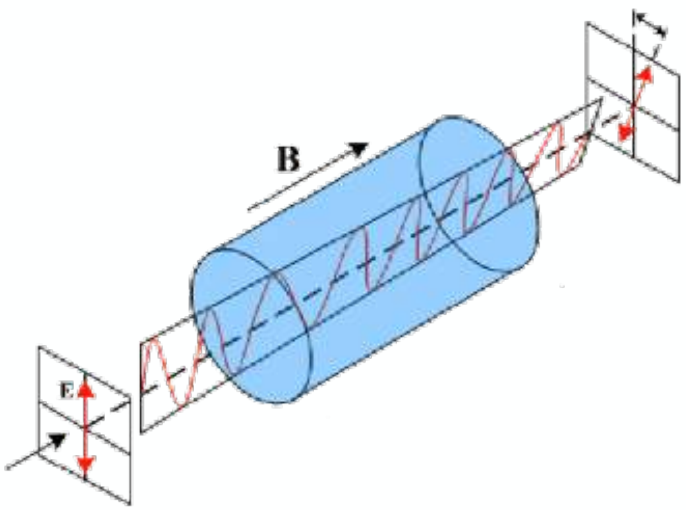

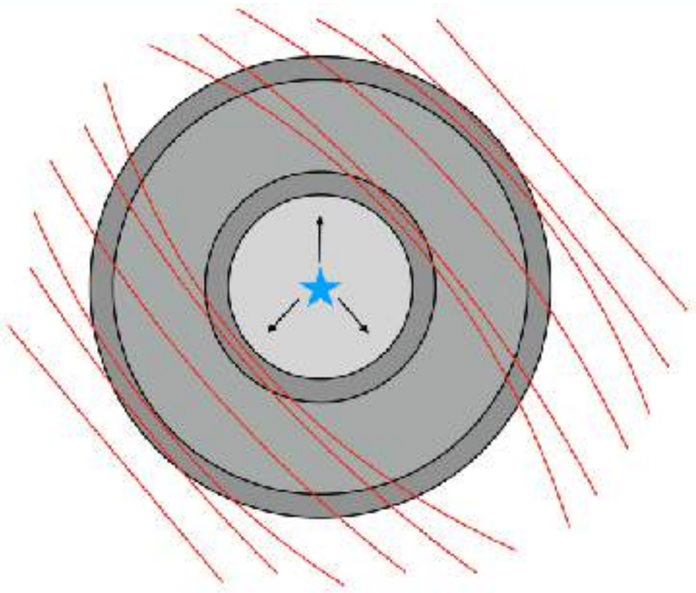

DUNLAP INSTITUTE *for* ASTRONOMY & ASTROPHYSICS

www.dunlap.utoronto.ca